

Effect of large amplitude oscillatory shear (LAOS) on the dielectric response of 1,4-*cis*-polyisoprene

S. Höfl^a, F. Kremer^b, H.W. Spiess^a, M. Wilhelm^{a,c,*}, S. Kahle^{a,*}

^a Max-Planck-Institute for Polymer Research, Ackermannweg 10, 55128 Mainz, Germany

^b Universität Leipzig, Institut für Experimentelle Physik I, Linnéstr. 5, 04103 Leipzig, Germany

^c Technische Universität Darmstadt, Institut für Maschinenbau, Hochschulstr. 1, 64289 Darmstadt, Germany

Received 10 February 2006; received in revised form 20 March 2006; accepted 24 March 2006

Available online 7 July 2006

Abstract

The dielectric response of 1,4-*cis*-polyisoprene under applied mechanical oscillatory shear with various shear amplitudes was investigated. For this purpose, a special setup was constructed which enables to measure dielectric spectra under the influence of large amplitude oscillatory shear (LAOS); the setup is explained in detail. A strong influence of the shear amplitude on the dielectric relaxation strength was observed if the dielectric normal mode was mechanically affected. With increasing amplitude the relaxation strength decreased while the mean relaxation time, the width and asymmetry basically remained unchanged. We interpret this process as an orientational phenomenon of the end-to-end-vectors which results in a decreasing fluctuation amplitude of the polarization fluctuations.

© 2006 Elsevier Ltd. All rights reserved.

Keywords: Dielectric spectroscopy; FT-rheology; Polyisoprene

1. Introduction

Rheology is a sensitive method to investigate mechanical relaxation of polymeric materials [1,2]. It gives qualitative information about viscosity, dynamics and molecular weight. In the linear regime of rheology the amplitude of the response is directly proportional to the amplitude of the imposed deformation. By applying large amplitude oscillatory shear (LAOS) the nonlinear regime is entered. The simple proportionality is lost and the interpretation of the rheological data is not anymore simple. To investigate the nonlinear behavior of materials under oscillatory shear, Fourier-Transform-Rheology was developed [3–6]. By analyzing the macroscopic stress signal by Fourier transformation this method allows to quantify the

mechanical nonlinearities in terms of intensity and relative phase of the generated higher harmonics [7].

In order to establish and quantify the relation between local molecular relaxation dynamics of polymers and macroscopic response to mechanical forces, it is necessary to correlate the LAOS response to a molecular perspective. The combination of LAOS and, *in situ*, dielectric spectroscopy fulfills this demand. Specifically, 1,4-*cis*-polyisoprene, a type-A polymer [8] allows to analyze the normal mode motion of the polymer chains via dielectric spectroscopy. This normal mode is assumed to be most influenced by LAOS, since the involved time scales are much longer compared to alpha- or beta-relaxation. The dielectric normal mode can be correlated to the longest relaxation time at the intersection point of G' and G'' of a linear oscillatory mechanical measurement [9]. Consequently, this type of polymer is highly suited to study the influence of LAOS on the dynamics of polymer chains via dielectric spectroscopy, and the polymer dynamics can be specifically quantified in terms of relaxation times, relaxation time distribution and dielectric strength. Needless to say that

* Corresponding authors. Tel.: +49 6131 379 209; fax: +49 6131 379 100.

E-mail addresses: wilhelm@mpip-mainz.mpg.de (M. Wilhelm), kahle@mpip-mainz.mpg.de (S. Kahle).

¹ Tel.: +49 6131 379 124; fax: +49 6131 379 100.

numerous examples exist, where mechanical and dielectric relaxation were both measured on the same polymer, [10] yet to our knowledge both techniques have not been applied simultaneously under oscillatory shear and in the nonlinear regime.

With this contribution we honor Prof. Pakula's work investigating the structure and dynamics in polymers and supramolecular systems using dynamic mechanical and dielectric spectroscopy [11] as well as X-ray scattering [12].

2. Theory

2.1. Dielectric spectroscopy

Under an applied, external electric field \vec{E} , electrical dipoles of molecules $\vec{\mu}$ are partially orientated in the direction of \vec{E} . This dipole orientation occurs via the motion of the molecules, allowing us to dielectrically observe this motion though the time-evolution of $\vec{P} \cdot \vec{P}$ is composed by the sum of all dipoles $\vec{\mu}$ in a unit volume

$$\vec{P} = \frac{1}{V} \sum_i \vec{\mu}_i + P_\infty \quad (1)$$

The molecular motion of the dipole $\vec{\mu}$ is not affected by the external electric field if the field intensity is sufficiently small, i.e. small compared with the local field fluctuations, and therefore linear dielectric responses observed for this case reflect the equilibrium motion. Israeloff directly proved this at the glass transition of glycerol [13].

In any real system the polarization is not a constant. Due to the motion (reorientation) of the particles the polarization fluctuates around a mean value $\langle P \rangle$. For homogeneous materials in equilibrium, the autocorrelation of the polarization fluctuations, c_p , is given by

$$c_p(\tau) = \frac{\langle \delta P(\tau) \delta P(0) \rangle}{\langle \delta P(0)^2 \rangle} \quad (2)$$

with $\delta P(\tau) = P(t) - \langle P \rangle$. In general, the dielectric features are examined for a material function, e.g. using the complex dielectric constant $\varepsilon^*(\omega)$ under an oscillatory electric field at an angular frequency ω . Through the Boltzmann superposition principle (valid for all linear phenomena), $\varepsilon^*(\omega)$ of the dipoles can be expressed in terms of $c_p(t)$ as

$$\varepsilon^*(\omega) = \varepsilon'(\omega) - i\varepsilon''(\omega) = \varepsilon_\infty - \Delta\varepsilon \int_0^\infty \frac{dc_p(t)}{dt} \exp[-i\omega t] dt \quad (3)$$

Here, $\varepsilon'(\omega)$ and $\varepsilon''(\omega)$ are the dynamic dielectric constant and loss, respectively. ε_∞ corresponds to the high frequency limit of the real part of $\varepsilon^*(\omega)$ and $\Delta\varepsilon$ is the dielectric relaxation strength.

2.2. Type-A polymers

According to Stockmayer [8], the dipoles of flexible polymer chains are classified into three types, where type-A and

type-B dipoles are connected with the chain backbone (parallel and perpendicular, respectively) and for type-C polymers the dipoles are attached to the side chain groups. In this article, we do not consider the (generally much faster) relaxation due to the type-B and type-C dipoles and focus our observation on the slow dielectric relaxation of the type-A chains, i.e. the global motion of the chain backbone. This motion results in the slow dielectric dispersion if the chains have the type-A dipoles aligned in the same direction, head-to-head to the chain backbone.

For this kind of dipoles, the polarization $\vec{P}(t)$ can be written in terms of the bond-vector \vec{u} of the sub-molecules (or monomer units) as

$$\vec{P}(t) = \mu_0 \sum_{\text{chain}} \sum_{n=1}^N \vec{u}(n, t), \quad (4)$$

with $\vec{\mu}_0$ the dipole moment of the sub-molecule (or monomer).

For 1,4-*cis*-polyisoprene as a type-A polymer, it is possible to measure different types of motion (or reorientation) for an amorphous homopolymer chain with dielectric spectroscopy and in particular its longest relaxation time. Of course, the longest relaxation time in the PI samples results from different faster types of motion, e.g., Rouse-modes, chain motion in presence of entanglements, constraint release and contour length fluctuations [14]. The dielectric spectrum of this motion is called normal mode and its frequency depends on the molecular weight [9,15–18]. The main part in the dielectric spectrum results from fluctuations of the end-to-end vector, and the peak maximum corresponds to the longest relaxation time. For comparison, in a mechanical spectrum this process is called the terminal mode.

Frequently, the dielectric function is analyzed by fitting the Havriliak–Negami function [19–21]

$$\varepsilon^*(\omega) = \varepsilon_\infty + \Delta\varepsilon \left(1 + i(\omega\tau_c)^b\right)^{-g}, \quad (5)$$

with τ_c the characteristic relaxation time, and b and g the shape parameters. b describes the width of the spectrum, g is the asymmetry parameter.

The dielectric spectra in this article (including the spectra measured under applied mechanical shear) are fitted by a superposition of a Debye- and a Cole–Davidson function:

$$\varepsilon^*(\omega) = \varepsilon_\infty + \frac{\Delta\varepsilon_1}{(1 + (i\omega\tau_D))} + \frac{\Delta\varepsilon_2}{(1 + (i\omega\tau_{CD}))^\beta}, \quad (6)$$

where β is the high frequency shape, $\tau_D = \tau$ the characteristic relaxation time, corresponding to the maximum frequency, $\Delta\varepsilon = \Delta\varepsilon_1 + \Delta\varepsilon_2$ the dielectric strength (the area under the whole peak in the ε'' vs. $\log \omega$ plot corresponding with the step height in the ε' vs. $\log \omega$ plot). With this fitting function we take into account that the normal mode spectrum results from different eigenmodes [22]. The first mode ($p=1$) can be fitted by a Debye-function. The modes of higher orders ($p=3, 5, 7, \dots$) have a diminishing intensity and the

Cole–Davidson-function is therefore a good choice to describe the total eigenmode spectrum.

2.3. FT-rheology

The fundamental theoretical aspects related to FT-rheology and the experimental realization have already been described in more detail in former publications [3–6,25]. Only a short summary will be given about the main arguments for the appearance of higher harmonics.

By applying oscillatory shear flow of shear rate $\dot{\gamma}$ (or oscillatory shear flow of angular frequency ω_1) the shear stress depends linearly to the shear rate (Newton's law) $\sigma = \eta \cdot \dot{\gamma}$.

If the viscosity depends on the absolute shear rate $|\dot{\gamma}|$ it can be expanded as a Taylor series using even exponents of shear rate:

$$\eta(\dot{\gamma}) = \eta_0 + a \cdot \dot{\gamma}^2 + b \cdot \dot{\gamma}^4 + \dots \quad (7)$$

For simplification one uses a complex notation. Inserting Eq. (7) in Newton's law we obtain an expression for the time dependent shear stress:

$$\begin{aligned} \dot{\gamma}(t) &\propto e^{i\omega_1 t} \\ \sigma(t) &\propto (\eta_0 + a \cdot \dot{\gamma}^2 + b \cdot \dot{\gamma}^4 + \dots) \dot{\gamma} \\ \sigma(t) &\propto \sum_{n=\text{odd}} a_n e^{i(n\omega_1 t + \varphi_n)}. \end{aligned} \quad (8)$$

The time dependent shear stress in Eq. (8) can be sorted by a magnitude Fourier transformation [23] into the frequency space where the different frequency components are resolved. The resulting spectrum has distinct peaks at odd multiples of the fundamental. Each peak is described by an amplitude a_n and a phase φ_n with $n = 3, 5, 7, \dots$ [6,24]. The degree of nonlinearity can be quantified as the ratio of the magnitude for the n th harmonic, $I(n\omega_1)$, with respect to the magnitude of the fundamental frequency, $I(\omega_1) : I_{3/1} = I(n\omega_1)/I(\omega_1)$. Correspondingly, the phase of a higher harmonic is defined as the relative contribution: $\Phi_n = \varphi_n - n \cdot \varphi_1$ [24].

To describe the dependence of $I_{3/1}$ with respect to the strain amplitude γ_0 the following empirical equation is used [25]:

$$I_{3/1}(\gamma_0) = A \left(1 - \frac{1}{1 + (B \cdot \gamma_0)^C} \right). \quad (9)$$

A is the maximum intensity of the relative third harmonic $I_{3/1}$, the plateau for large shear amplitudes. Its value is typically 0.2 ± 0.1 . B is the critical inverse strain amplitude (when $\gamma_0 = 1/B$ then $I_{3/1} = A/2$) and C is the power-law dependence for small strain amplitudes, being in the range of 2.

3. Experimental

3.1. Setup

For the experiments a new setup was built using a combination of the ARES-Rheometer (TA Instruments) and the dielectric ALPHA-Analyzer (Novocontrol Technologies, Hundsangen, Germany). Both instruments provide highest resolution and sensitivity.

The ALPHA-Analyzer is able to measure 12 orders of magnitude frequency range (3×10^{-5} Hz – 2×10^7 Hz), 16 orders of impedance range (10^{-2} Ω – 10^{14} Ω) and 15 orders of capacity range (10^{-15} F – 1 F). These ranges exceed the capacitance bridges used in former rheo-dielectric measurements by several decades in each quantity [26,27]. The new setup allows a $\tan \delta$ resolution of $\pm 3 \times 10^{-5}$ to $\pm 10^{-3}$, depending on the used capacity.

The ARES-rheometer is equipped with a 1KFRTN1 torque transducer (detection of torques within 4×10^{-7} Nm – 0.1 Nm). An external PC with the TA Orchestrator Software controls the ARES, and the data for FT-rheology are executed by a home written Labview routine. An additional PC controls the ALPHA-analyzer with the Novocontrol windeta software. The oven of the rheometer suits as sample cell for the rheological and the rheo-dielectric measurements (see Fig. 1). This guarantees temperature control and additional electric shielding against the environment, specifically electronic noise.

The sample is between two parallel plates 15 mm in diameter. These geometries are electrically connected to the ALPHA-analyzer to monitor dielectric spectra during shear experiments.

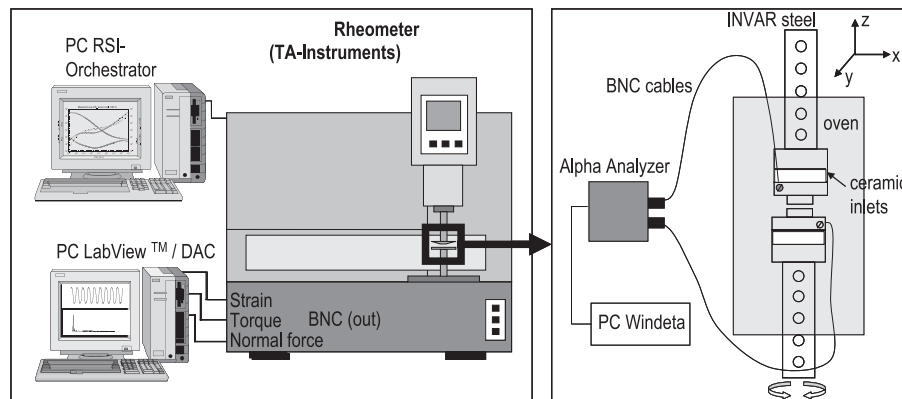


Fig. 1. Experimental setup, the combination of a rheometer and a dielectric analyzer *in situ*. The coordinate system shows the shear direction (x, y) and the direction of the applied electric field (z).

To realize these connections new fixtures and geometries had to be drafted and constructed. Technical details will be published subsequently. For this, INVAR steel with an extremely low temperature coefficient of $1.3 \times 10^{-6} \text{ K}^{-1}$ (in comparison to $13 \times 10^{-6} \text{ K}^{-1}$ in conventional steel) was used. This setup allowed to fix BNC-cables which lead out of the oven and to the analyzer. Electrode and fixture are separated by ceramic insulations as shown in Fig. 1. The thickness of the sample between the two plates was 0.1 mm.

3.2. Samples

The samples were anionically synthesized [28] linear 1,4-*cis*-polyisoprenes (PI) with similar molecular weight and low polydispersity (see Table 1). For the measurements bulk polymers were used. Their microstructure (about 90% 1,4-conformation with over 60% amount of *cis* conformation) was verified with ^1H and ^{13}C NMR. To avoid additional conductivity by impurities of the samples the possible Li^+ content remaining from the synthesis was carefully removed by precipitating with methanol.

4. Results

4.1. Rheology

To characterize the rheological behavior of our polymers we measured each sample at different temperatures and in the frequency range of 0.02 to 15 Hz. The G' and G'' data were shifted using the time-temperature-superposition (TTS)-principle to construct mastercurves to gain a resulting frequency range of 4×10^{-1} to 2×10^5 Hz. Fig. 2 shows an example of this mastercurve relative to a reference temperature of 283 K for the PI 55 sample.

At this temperature the intersection point of G' and G'' is at 11.45 Hz. For the sample PI 80 the characteristic temperature and frequency extracted from its mastercurve (not shown here) is referred to 298 K, and 8.24 Hz. These characteristic values are taken for the mechanical shear rate of the rheo-dielectric measurements.

The measurement conditions (temperature and frequency) were slightly changed due to the different molecular weights. It is desirable to have the maximum frequency in the range between 1 Hz and 10 Hz and a temperature above T_g . Using these requirements the measurement conditions are chosen accordingly.

The rheological properties (G'' as a function of shear amplitude, normalized to G'' at $\gamma_0 = 0.2$) during the rheo-dielectric experiments are given in Fig. 3. The loss module G'' shows

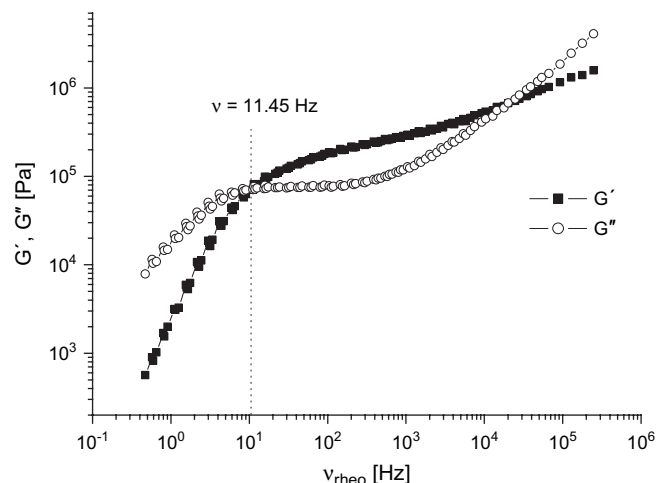


Fig. 2. Mastercurve for the shear moduli (G' , G'') for PI 55. The reference temperature is 283 K. The strains for the different frequency sweeps incorporated in the mastercurve were between 0.0025 and 0.004.

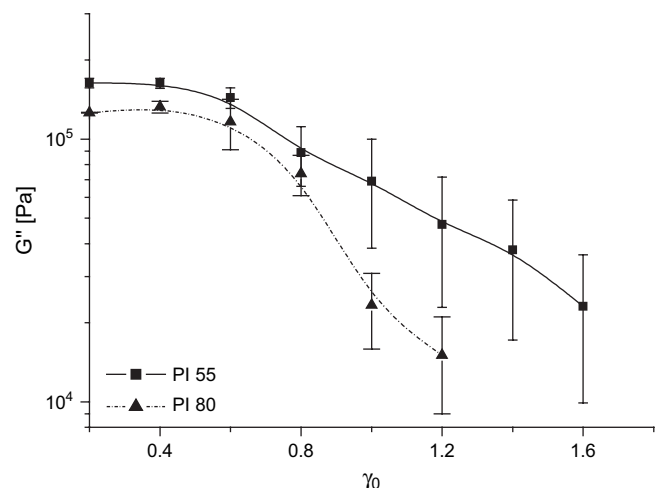


Fig. 3. G'' as a function of γ_0 ($0 \leq \gamma_0 \leq 1.6$) at $T = 283 \text{ K}$ and $\nu_{\text{mech}} = 11.45 \text{ Hz}$ (PI 55), $T = 298 \text{ K}$ and $\nu_{\text{mech}} = 8.24 \text{ Hz}$ (PI 80).

a decrease of almost one order of magnitude as a function of strain amplitude when the nonlinear regime is entered. Note, that G' shows under these conditions the same behavior as G'' .

A quantitative measure of the nonlinearity is given by the amplitude of the third harmonic $I_{3/1}$. A significant intensity for the nonlinearity is assumed above $I_{3/1} = 0.5\%$. Fig. 4 shows the intensity of the third harmonic as a function of shear amplitude for the two samples. Note, that the measurement conditions were slightly changed with respect to temperature and frequency for each sample. For reliable results in FT-rheology the frequency should not be higher than 2 Hz; otherwise the signal-to-noise ratio decreases. Thus, we chose temperatures as 268 K (PI 55), 293 K (PI 80); the frequency was 1.6 Hz (PI 55 and PI 80).

The third harmonic $I_{3/1}$ of PI 55 and PI 80 has a very similar behavior, increasing from close to 0% to approximately 1.6% at a γ_0 of 1. $I_{3/1}$ of the PI 80 sample is slightly higher than for

Table 1
Characteristics of the investigated samples

Name	M_w (kg/mol)	M_w/M_n	T_g ($^{\circ}\text{C}$)
PI 55	54.8	1.03	-63
PI 80	79.1	1.04	-64

Both samples are 1,4-*cis*-polyisoprenes with a narrow distribution M_w/M_n and the glass transition temperature measured by DSC.

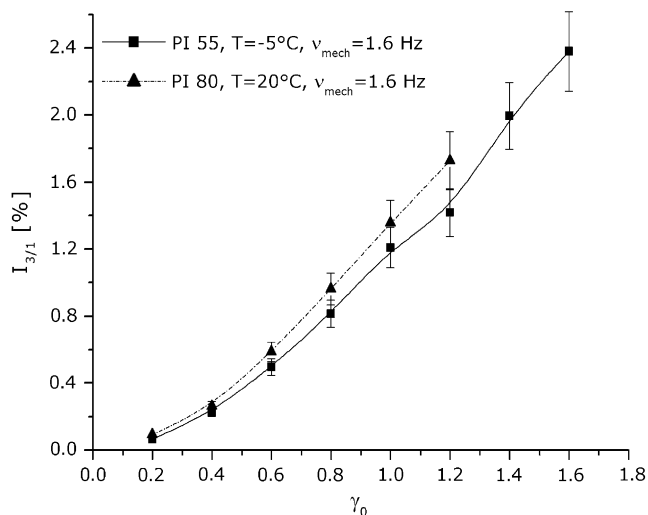


Fig. 4. The intensity of the mechanical third harmonic $I_{3/1}$ to quantify the degree of nonlinearity as a function of shear amplitude. The measurement conditions were 268 K, 1.6 Hz (PI 55), 293 K, 1.6 Hz (PI 80).

PI 55, corresponding to a slightly higher influence of the shear deformation.

It should be noted that nonlinear spectroscopy is very sensitive to sample details. This became evident when one commercial sample of similar molecular weight with linear and nonlinear rheology was investigated. This sample (not shown here) had a completely different response as the specifically synthesized samples. There are several origins for this difference. For instance, the commercial sample contained a stabilizer which is not present in the samples studied here (the measurements are performed under nitrogen atmosphere and a degradation of the sample was not observed after the experiment using mechanical measurements). Such additives could have an influence on the response of the polymer. Second, the microstructure, i.e. 1,2- 1,4-, *cis*- or *trans*-configuration, influences the mechanical behavior (but there was no difference seen within the investigated samples). Further, even low amounts of crosslinking or branching that are not seen in linear rheological measurements could be visible in the nonlinear regime [29].

4.2. Dielectric spectroscopy

As a next step the dielectric spectra at the characteristic temperatures were measured to investigate if the normal mode peak is at the position corresponding to the mechanical terminal frequency. The results for PI 55 ($T = 283$ K) and PI 80 ($T = 298$ K) are shown in Fig. 5. We observe the normal mode peak between 1 and 10 Hz in accordance to mechanical spectroscopy.

The longest relaxation time τ is taken from the Debye-function and can be calculated from the angular frequency ω_{\max} of the position of the maximal loss ε'' by [9] $\omega_{\max} = 1/\tau$. The results for the normal mode analysis spectra are given in Table 2. Fig. 6 shows an example for a fit of a normal mode peak (PI 55, $T = 283$ K, $\gamma_0 = 0.4$).

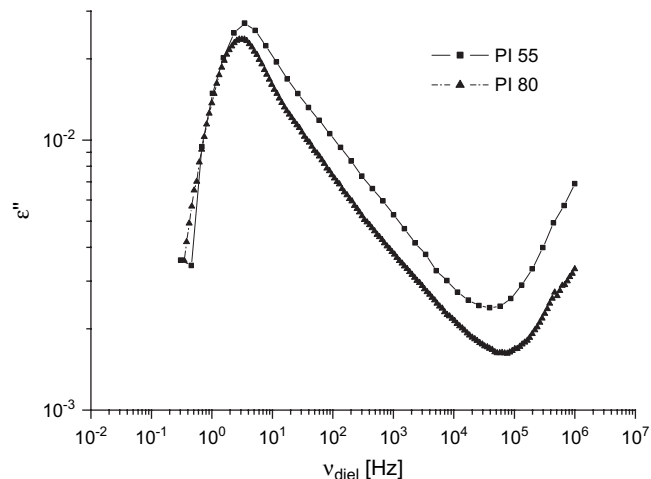


Fig. 5. Normal mode spectra from dielectric spectroscopy for PI 55 ($T = 283$ K) and PI 80 ($T = 298$ K).

4.3. Rheo-dielectric spectroscopy in combination with LAOS

Fig. 5 shows the imaginary part of the dielectric function (without shear) for the two different samples. Fig. 7 shows the dielectric spectra with different shear amplitudes for the PI 55 sample. For the shear deformation we use a frequency of 11.45 Hz. This frequency corresponds to the intersection point of G' and G'' in the linear regime at this temperature.

We observe clearly a decreasing intensity of the dielectric spectrum with increasing shear amplitude. The peak position and the shape, however, remain (at least to a good approximation) unchanged.

The inset in Fig. 7 displays the results in a different way. $\Delta\varepsilon$ vs. the nonlinearity $I_{3/1}$ indicates that $\Delta\varepsilon$ decreases with higher nonlinearities (i.e. higher strain amplitudes) to a certain constant level.

The behavior of the sample with higher molecular weight (PI 80) was similar (data not shown).

As described in the previous section, the dielectric measurements were fitted with a superposition of two functions,

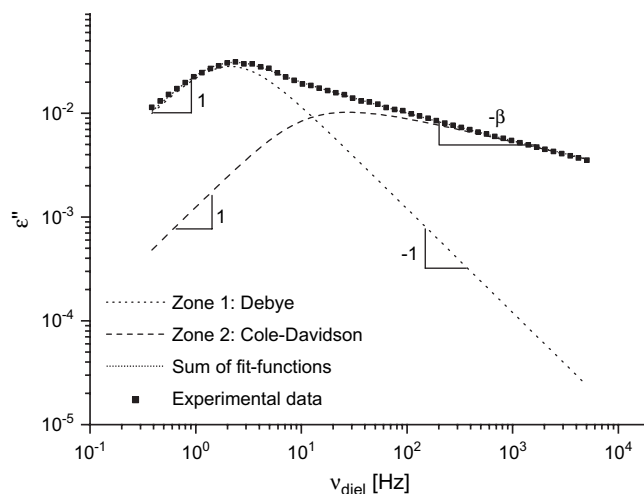


Fig. 6. Example for a normal mode peak fitted by a superposition of a Debye- and a Cole-Davidson-function (PI 55, $T = 283$ K, $\gamma_0 = 0.4$).

Table 2
Results of the fitting with Debye- and Cole–Davidson-function (Eq. (12))

γ_0	PI 55		PI 80	
	β	τ (s)	β	τ (s)
0	0.262	0.310	0.267	0.333
0.2	0.257	0.305	0.265	0.327
0.4	0.258	0.295	0.263	0.332
0.6	0.256	0.302	0.222	0.335
0.8	0.234	0.321	0.256	0.328
1	0.252	0.315	0.269	0.338
1.2	0.236	0.310	0.256	0.336
1.4	0.246	0.352		
1.6	0.254	0.372		
Estimated error (%)	± 10	± 10	± 10	± 10

τ is the characteristic relaxation time, β describes the asymmetry of the normal mode peak.

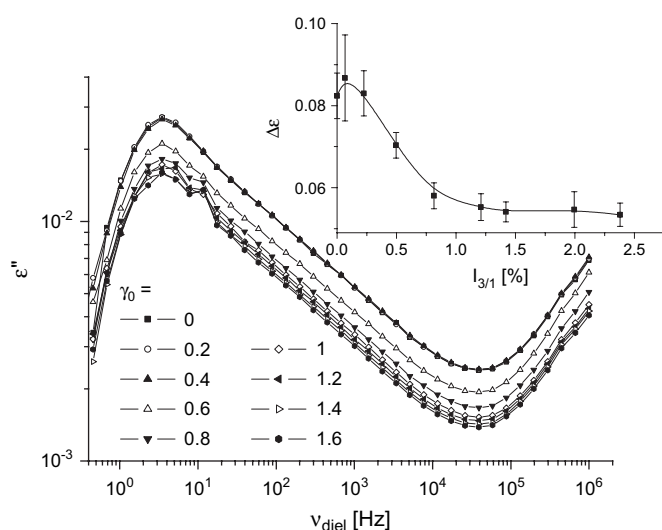


Fig. 7. Dielectric spectra taken under mechanical shear (PI 55) for strain amplitudes between $0 \leq \gamma_0 \leq 1.6$. The temperature was 283 K, the frequency of the mechanical oscillatory shear was 11.45 Hz. The inset shows the dielectric strength $\Delta\epsilon$ as a function of $I_{3/1}$.

one Debye- and one Cole–Davidson-function (see Eq. (6)). The results are listed in Table 2.

The samples can be compared in the combined rheo-dielectric measurements since similar trends for all the samples are achieved.

Within the experimental errors the high frequency shape, β , is within measurement errors independent of strain amplitudes and there is even no difference between the parameters taken from the dielectric spectrum without shear and the spectra monitored under shear ($\beta \approx 0.25$ for all strains and samples). Additionally, the characteristic relaxation time, τ , is within experimental errors (about 10%) independent of shear amplitude. In PI 55 a change of about 15% is visible between a strain amplitude of 1.6 and the spectrum without shear. PI 80 does not show a change for τ , but for mechanical stability the strain amplitudes $\gamma_0 = 1.4$ and $\gamma_0 = 1.6$ are not accessible. The dielectric relaxation time τ is for both samples approximately one order of magnitude lower than the relaxation times extracted from the rheological data. But both dielectric and mechanical

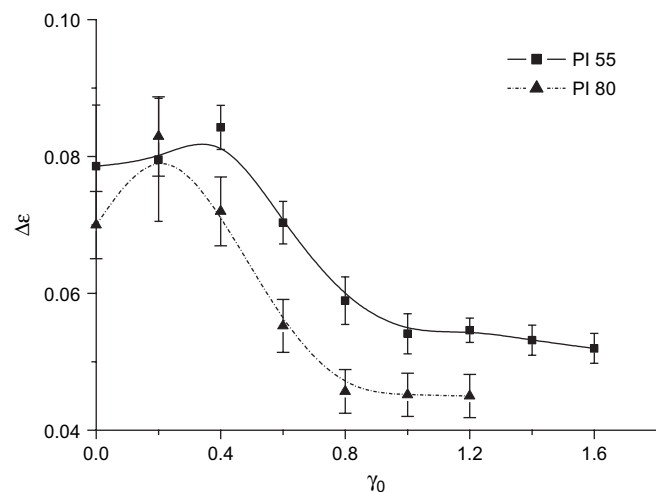


Fig. 8. Dielectric strength $\Delta\epsilon$ for both PI samples as a function of shear amplitude.

measurements show the expected scaling exponent 4 as a function of molecular weight.

This means, that LAOS does not influence the relaxation time and the spectrum of the normal mode process. This analysis confirms what is already approximately visible in the dielectric spectra (Fig. 7).

In contrast to the presented parameters the dielectric strength, $\Delta\epsilon$, shows a significant change during oscillatory shear (Fig. 8).

The difference between an undisturbed spectrum and a spectrum monitored under small shear amplitudes (< 0.4) is negligible. For strain amplitudes between $\gamma_0 = 0.4$ and $\gamma_0 = 1$ the dielectric strength decreases rapidly by around 40%. For higher shear amplitudes, $\Delta\epsilon$ levels off. The decrease of 40% is a factor of 4 more than found in former studies on polyisoprene in solution [27]. However, in this work an entangled 10% polyisoprene ($M_w > 1000$ kg/mol) solution under steady shear was investigated. There, the highest shear rate was three orders of magnitude higher than the inverse of the longest relaxation time.

5. Discussion

The combination of oscillatory rheology and dielectric spectroscopy performed on a model type-A polymer, 1,4-*cis*-polyisoprene, enabled the investigation of end-to-end-vector relaxation under mechanical deformation. The first results shown in this article refer to the terminal mode.

The experimental situation is the following: the sample is deformed in the x – y direction, while for measuring the dielectric response only the z direction is relevant. In other words, only the dipole moment component which is parallel to the applied electrical field along the z direction contributes to the polarization. For the undisturbed system the end-to-end vectors of the polymer chains are assumed to be equally distributed in all directions. Upon shearing the sample this distribution becomes anisotropic and can be visualized by an oriented ellipsoid, that is stretched in x – y direction and compressed in z direction. Due to the type-A nature of 1,4-*cis*-polyisoprene (dipole

moment parallel to the chain backbone) the same stretching and compression happens with the resulting dipole moment, and the polarization in z direction decreases. This is only valid for the distribution of end-to-end vectors, not for the conformations of the segments of the polymer chains, which are of course not equally distributed in a sphere, see e.g. Ref. [30]. Please note, that this is a static picture which can be supported by recent molecular dynamic computer simulations [31].

For dynamic analysis only the fluctuations in the z direction are important. From the fluctuation–dissipation theorem (FDT) we know that the dielectric relaxation strength is proportional to the mean square of the fluctuation of the polarization $\langle \delta P^2 \rangle \propto \Delta \epsilon$ [9]. This explains qualitatively the decrease of $\Delta \epsilon$ with increasing force amplitudes as seen in Fig. 7.

In Section 4.3 we have observed that LAOS has a strong influence on the dielectric relaxation behavior. Surprisingly, it seems that not only the dynamics of the whole polymer chain is affected but also the segmental motion (glass transition). This becomes clear if we observe the low frequency flank of the glass transition peak (see Fig. 7). We expect that the glass transition spectrum (being much faster than the normal mode process) should not be influenced by such a slow mechanical shear. Its relaxation strength, however, is also lowered by mechanical shear. This means, that the force changes the topology not only on the length scale of the polymer coil but also on the length scale of a few polymer segments.

6. Conclusion and outlook

The overall chain dynamics of 1,4-*cis*-polyisoprene was investigated by two different experiments separately and in combination. It is to our knowledge the first time that oscillatory shear and broadband dielectric spectroscopy is performed *in situ* on polyisoprene melts in the nonlinear regime. By applying large amplitude oscillatory shear (LAOS) we observe increasing mechanical nonlinearities with higher shear amplitudes. This becomes clear in the decreasing loss modulus G'' , the increasing intensity of the third harmonic $I_{3/1}$ measured by FT-rheology and the decreasing dielectric strength $\Delta \epsilon$ measured by rheo-dielectrics. The setup for the rheo-dielectric measurements was specifically constructed and is – to the best of our knowledge – unique in terms of resolution and the possibility to perform oscillatory shear.

The decreasing intensities of $\Delta \epsilon$ correspond to a decreasing fluctuation amplitude of the end-to-end vector of the spontaneous fluctuations. This was also discussed as a slight orientation of the end-to-end vector in the x – y plane.

Specifically anionically synthesized PI samples were measured. The increasing mechanical nonlinearity is visible in all of them. This is qualitatively monitored by linear rheology, FT-rheology and rheo-dielectrics. In a next step, rheo-dielectrics should be performed also at the α -process to investigate the dielectric relaxation spectrum under shear at much higher frequencies beyond the maximum of the α -peak. The question arises if mechanical force also influences the local orientation of only a few polymer segments. Further, the molecular weight dependence of the dielectric response

on mechanical deformation is an interesting feature that has to be analyzed. In upcoming projects the influence of microstructure which plays an important role in rheological experiments and the dependence of mechanical frequency will be investigated by rheo-dielectrics. It should be possible to correlate quantitatively these results with numerical molecular modeling under oscillatory shear.

Acknowledgement

The authors thank Piotr Minkin for his help in constructing the setup and V. Maus and M. Drechsler for synthesizing the polyisoprene samples. S.H. thanks the MPG for financial support.

References

- [1] Larson GL. The Structure and rheology of complex fluids. Oxford: Oxford University Press; 1999.
- [2] Macosko CW. Rheology – principles, measurements and applications. New York: Wiley-VCH Inc; 1994.
- [3] Giacomin AJ, Dealy JM. Large amplitude oscillatory shear. In: Collyer AA, Clegg DW, editors. Rheological measurements. London: Chapman and Hall; 1998.
- [4] Krieger IM, Niu TF. Rheol Acta 1973;12:567–71.
- [5] Wilhelm M, Maring D, Spiess HW. Rheol Acta 1998;37(4):399–405.
- [6] Wilhelm M, Reinheimer P, Ortseifer M. Rheol Acta 1999;38(4):349–56.
- [7] Wilhelm M, Reinheimer P, Ortseifer M, Neidhöfer T, Spiess HW. Rheol Acta 2000;39:241–6.
- [8] Stockmayer WH, Burke JJ. Macromolecules 1969;2(6):647–50.
- [9] Kremer F, Schönhals A. Broadband dielectric spectroscopy. Berlin: Springer; 2003.
- [10] McCrum NG, Read BE, Williams G. Anelastic and dielectric effects in polymeric solids. New York: Dover; 1991.
- [11] Pakula T, Geyler S, Edling T, Boese D. Rheol Acta 1996;35(6):631–44.
- [12] Fischbach I, Pakula T, Minkin P, Fechtenkötter A, Müllen K, Spiess HW, et al. J Phys Chem B 2002;106(5):6408–18.
- [13] Israeloff NE. Phys Rev B 1996;53(18):11913–6.
- [14] Doi M, Edwards SF. The theory of polymer dynamics. Oxford: Clarendon Press; 1986.
- [15] Boese D, Kremer F, Fetters LJ. Macromolecules 1990;23(6):1826–30.
- [16] Boese D, Kremer F, Fetters LJ. Polymer 1990;31:1831–7.
- [17] Schönhals A. Macromolecules 1993;26(6):1309–12.
- [18] Abdel-Goad M, Pyckhout-Hintzen W, Kahle S, Allgaier J, Richter D, Fetters LJ. Macromolecules 2004;37(21):8135–44.
- [19] Havriliak S, Negami S. Polymer 1967;8(4):161–210.
- [20] Adachi K, Kotaka T. Macromolecules 1985;18(3):466–72.
- [21] Imanishi Y, Adachi K, Kotaka T. J Chem Phys 1988;89(12):7585–92.
- [22] Watanabe H. Macromol Rapid Commun 2001;22(3):127–75.
- [23] Ramirez RW. The FFT fundamentals and concepts. Engelwood Cliffs: Prentice-Hall; 1985.
- [24] Neidhöfer T, Wilhelm M, Debbaut B. J Rheol 2003;47(6):1351–71.
- [25] Wilhelm M. Macromol Mater Eng 2002;287(2):83–105.
- [26] Watanabe H, Sato T, Matsumiya Y, Inoue T, Osaki K. Nihon Reoroji Gakkaishi 1999;27(2):121–5.
- [27] Watanabe H, Ishida S, Matsumiya Y. Macromolecules 2002;35(23):8802–18.
- [28] McGarth JE, editor. Anionic polymerisation – kinetics, mechanisms, and synthesis. Washington D.C.: American Chemical Society; 1981.
- [29] Höfl S. Ph.D. thesis, Universität Mainz; 2006.
- [30] Everaers R, Sukumaran SK, Grest GS, Svaneborg C, Sivasubramanian A, Kremer K. Science 2004;303(5659):823–6.
- [31] Svaneborg C, Grest GS, Everaers R. Phys Rev Lett 2004;93(25):257801–4.